




# Phase modulation using a titanium dioxide strip on lithium niobate

XIAOFENG ZHU,<sup>1,\*</sup> SEAN NELAN,<sup>1,2</sup>  ANDREW J. MERCANTE,<sup>2</sup> BENJAMIN SHOPP,<sup>2</sup> PENG YAO,<sup>2</sup> SHOUYUAN SHI,<sup>1,2</sup> AND DENNIS W. PRATHER<sup>1,2</sup>

<sup>1</sup>Electrical and Computer Engineering Department, University of Delaware, Newark, DE 19716, USA

<sup>2</sup>Phase Sensitive Innovations, Inc., 116 Sandy Dr, Newark, DE 19713, USA

\*xzhu@udel.edu

**Abstract:** In this manuscript, we demonstrate the first phase modulator using titanium dioxide as a strip loaded waveguide on thin-film lithium niobate. The amorphous titanium dioxide was fabricated using RF reactive sputtering followed by a dielectric lift-off process. Two gold electrodes were deposited next to the waveguide by using the same process. This process eliminates the need for plasma etching or high-temperature vapor deposition methods, opening the door to fabrication on sensitive material systems. A propagation loss of 0.156 dB/mm and  $V_{\pi}$  of 3.2 V at 1550 nm were experimentally measured and reported.

© 2022 Optica Publishing Group under the terms of the [Optica Open Access Publishing Agreement](#)

## 1. Introduction

Thin-film lithium niobate on insulator (TFLNOI) is well-established as the material of the future of photonic integrated circuits (PICs) for its desirable optical and physical properties. Lithium niobate has a broad transparency window in at telecom wavelengths, a high refractive index, a high electro-optic coefficient ( $r_{33}=31.8\text{pm/V}$ ) and a low third-order non-linearity [1], which make it an ideal material for electro-optical modulation [2] and fiber-optic EO-switching [3], which are essential components of modern telecommunications.

Silicon (Si) and silicon nitride ( $\text{SiN}_x$ ), have been investigated as candidates to use as the strip-loaded waveguide in previous work [4,5]. However, silicon has much higher refractive index than lithium niobate and a third-order non-linearity three magnitudes higher, which causes low mode confinement within the lithium niobate layer and undesirable distortion at high optical power.  $\text{SiN}_x$  has a lower refractive index (1.94) but is unable to support tight bending radii needed for compact device footprints. In this work, we report on the use of titanium dioxide ( $\text{TiO}_2$ ) as a strip-loading material. Due to its relatively higher refractive index ( $n=2.337$ ) than lithium niobate and broad transparency window, it is shown to be an ideal candidate and the material of choice. Moreover, titanium dioxide is an easily-obtained material in laboratories; it can be made by Sol-gel [6], RF reactive sputtering [7,8], and atomic layer deposition (ALD) [9]. What's more, titanium dioxide has negative thermal optic coefficient (OTC) of  $-2.15 \cdot 10^{-4} \text{K}^{-1}$  [10,11], which opposes that of lithium niobate to create a more thermally-stable device in comparison to silicon nitride. The  $\text{TiO}_2$ -on-TFLNOI shows potential for athermal modulator design [12]. The attractive optical and physical properties of  $\text{TiO}_2$  make it a strong candidate for numerous application.

Finally, the fabrication process for the titanium dioxide material system is simplified considerably in comparison to a ridge-etched TFLNOI waveguide or a  $\text{SiN}_x$  strip-loaded waveguide deposited by plasma-enhanced chemical vapor deposition (PECVD) or low-pressure chemical vapor deposition (LPCVD). The lift-off process used in this work excludes the need for high-temperature processing, but yields an extremely stable wave-guiding structure with potential for athermal operation.

In this work, we report a DC-Phase modulator operating at 1550 nm using a TiO<sub>2</sub>-on-TFLNOI strip-loaded waveguide and sputtered gold electrodes. The phase modulator was designed using commercial software, ANSYS Lumerical MODE and ANSYS High Frequency Structure Simulator (HFSS). A simple bi-layer dielectric lift-off process has been used to fabricate both the TiO<sub>2</sub> waveguide and electrodes. The lift-off process can minimize the surface roughness caused by the fabrication process, which is considered to be the primary cause of the propagation loss of the TiO<sub>2</sub> waveguide. [13] Both waveguide and electrode materials were deposited in an RF sputter system. The optical loss and half-wave voltage of the fabricated device were experimentally characterized. To the best of our knowledge, this is the first time an EO-phase modulator has been demonstrated in the TiO<sub>2</sub> on TFLNOI material platform, and the lowest reported optical propagation loss for a TiO<sub>2</sub> strip-loaded waveguide.

## 2. Design

An optical simulation has been performed by using ANSYS Lumerical Mode simulation, as shown in Fig. 1(a), majority of the mode confined in the LN layer. A single mode TiO<sub>2</sub>-on-TFLNOI waveguide with optical group index ( $n_g$ ) of 2.21 at 1550 nm was simulated. Fig. 1(e) Two sweeps have been run to optimize the mode profile, one to assess confinement in LN and one to assess mode size optimization of which lead to better modulation efficiency.

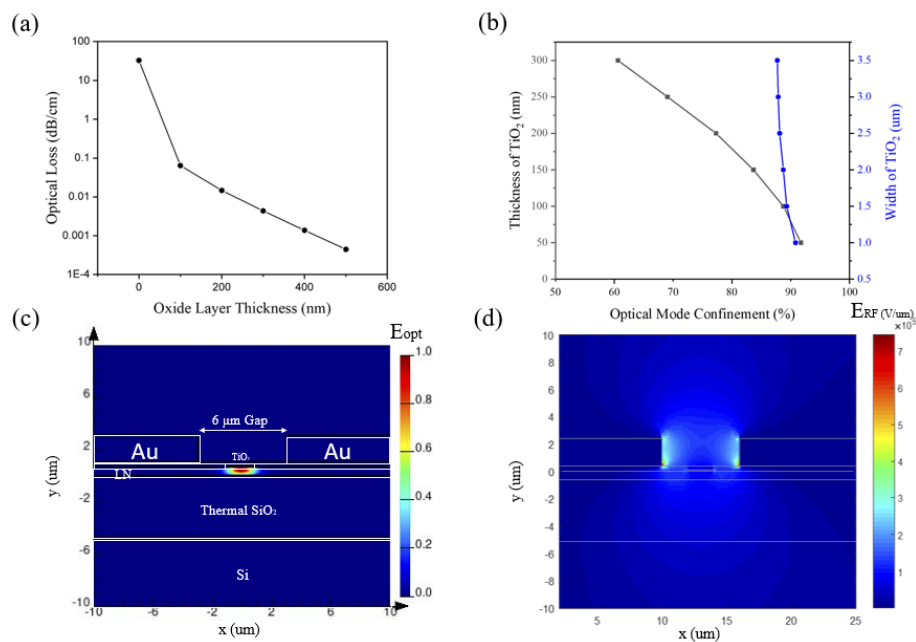


**Fig. 1.** a: Simulation results of cladding silicon dioxide layer vs optical loss. b: The black line shows thickness of TiO<sub>2</sub> vs mode confinement and the blue line shows the width of TiO<sub>2</sub> vs the mode confinement in LN layer. c: The cross section of Optical mode simulation result. d: HFSS simulation result of cross-section of RF electric field distribution within the designed device.

As Shown in Fig. 1(b), the mode confinement slightly changed from 87.71 % to 90.82 % while the width of the waveguide decreased from 3.5 μm to 1 μm. Since the mode confinement not vary a lot from 1 μm to 2 μm, a 2 μm wide of TiO<sub>2</sub> strip has been chosen as actual dimension for an easier fabrication process. The 2 μm wide waveguide allows using photomask for lithography. The thickness of the loading strip is the critical parameter that determines how much of the

mode confined within the lithium niobate layer. For a better phase modulation, high mode confinement in Lithium niobate layer need to be achieve.  $\text{TiO}_2$  has slightly higher optical index than lithium niobate, more optical mode will shift into lithium niobate layer with thinner  $\text{TiO}_2$  layer. Considering some physical constraints and the surface roughness caused by the thickness of  $\text{TiO}_2$ . Thicker  $\text{TiO}_2$  will have higher surface roughness, which will contribute additional scattering loss [14], a 100 nm thickness of  $\text{TiO}_2$  would be sufficient for this modulator design. Based on the simulation results, 86 % mode was confined in the lithium niobate layer with a mode size of  $1.9 \text{ } \mu\text{m}^2$ , shown in Fig. 1 (c). Additionally a silicon dioxide layer is added into the simulation to reduce the optical loss caused by metal absorption, shown in Fig. 1(a). Based on the simulation result, 100 nm silicon dioxide has reduced the optical loss from 10 dB/cm to 0.1 dB/cm. However, align 2 cm long optical waveguide with 1.6 cm long gold electrode with a narrow 6  $\mu\text{m}$  is reach the capability of this instrument. A slightly thicker silicon dioxide would make the alignment process more forgivable. Too thick of silicon dioxide layer affects the modulation efficiency, while the electro magnetic wave generated by electrodes travels from lower refractive index silicon dioxide into high refractive index lithium niobate region. 400 nm PECVD silicon dioxide would be sufficient to reduce the impact from metal absorption while maintains the modulation efficiency, shown in Fig. 1(b). A thicker cladding layer is also helpful for the polishing and light coupling process. E-beam lithography can be considered for aligning waveguide and electrode for a narrower gap in future work, it can significantly improve the modulation efficiency and reduce  $V_\pi$ . The HFSS simulation shown in Fig. 1(d) is purely used to estimate the optical and RF electric field overlap. This performance of  $\text{TiO}_2$ -on-TFLNOI platform can be improved by optimizing the design of thermal stability and high-speed electrodes.

### 3. Fabrication

The fabrication of optical waveguide started with a silicon handle 700 nm X-cut single crystal thin-film-lithium-niobate provided by NanoLN. The surface was cleaned by piranha solution for 1 min and 5 mins oxygen plasma to achieve an ultra-clean surface condition before lithography process. As shown in Fig. 2(a) LOR5A photoresist was spun at 6000 RPM for 1 min and baked for 5 mins at 300 °C. AZ1512 was spun at 3000 RPM for 1 min and baked for 3 mins at 95 °C to reach bi-layer photoresist profile. In order to keep good contact between photoresist layer and photo-mask, edge remover was applied. The waveguide pattern was created by exposing under 365 nm light with the i-line filter. After the developing process, a RF  $\text{TiO}_2$  reactive sputtering deposition at room temperature was carried out. The gas recipe was set to 10:3 for Ar:  $\text{O}_2$  to control the quality and deposition rate of the  $\text{TiO}_2$ , where Ar is the working gas and  $\text{O}_2$  is the reactive gas. High Ar gas will only deposit Ti, high  $\text{O}_2$  flow rate will slow down the deposition rate, which will increase the deposition time. The current deposition process takes 4 hours for 100 nm  $\text{TiO}_2$  deposition. The solution for increasing the deposition rate but not affecting the material quality is introduce a dual-target deposition [15]. After the deposition, the sample was soaked into remover PG for 30 mins followed by 5 mins ultrasonic to remove the bi-layer photoresist. a 400 nm low refractive index plasma-enhanced chemical vapor deposition (PECVD) silicon dioxide ( $n=1.44$ ) was deposited to avoid any other source of contamination and reduce the metal absorption. The same bi-layer process was carried out once again for electrode deposition. Electrode patterns aligned with a 2 cm long waveguide with 6  $\mu\text{m}$  gap and 300 nm thickness by using laser writer, shown in Fig. 2(C). The sample was then spin coat by 8  $\mu\text{m}$  NR2-8000 spin at 3000 RPM. Dicing and 15 degree angel polishing were carried out to from a smooth and clean facet for light coupling. Since the silicon dioxide layer can also be done in sputtering, by using silicon dioxide target, this device could be completed only by sputter and optical lithography which significantly reduces the fabrication steps and costs.

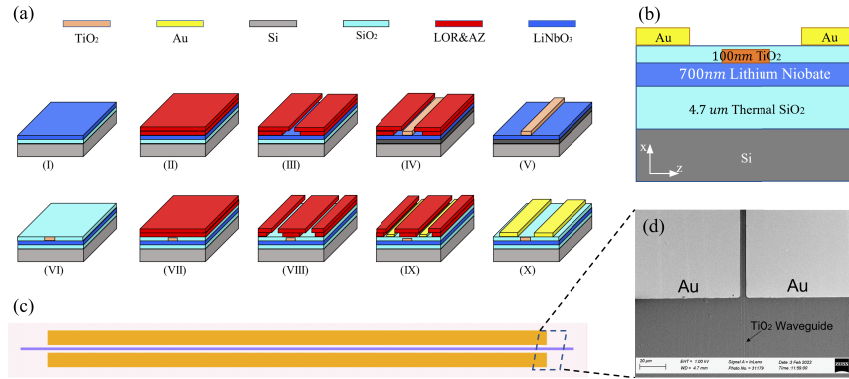


**Fig. 2.** a: Flow chart of the TiO<sub>2</sub>-on-TFLN phase modulator fabrication process. b: Cross-section of the device layout. c: Overview layout of electrodes and waveguides. d: SEM image of a fabricated device's waveguide and interaction regions.

#### 4. Characterization

Both optical and electro-optic properties of this phase modulator have been characterized. The propagation loss of 19 fabricated waveguides was measured by Optical Backscatter Reflectometer (OBR) at 1550nm. In Fig. 3(a), the OBR continually measures the back-scattering from the entire waveguide. As shown in Eq. (1), Loss calculation can be done by substrate the output power from input and divide by the length of the waveguide, which is around 1.5 dB/cm in this 2 cm long waveguide. Another way is to choose two regions from the head and tail of the plot, averaging 1 mm wide data point to eliminate the noise floor impact and calculate the slope, the propagation loss of 1.56 dB/cm was measured. Peak to peak measurement matches well with the slope calculation.

$$\alpha = \frac{P_{in} - P_{out}}{L} \quad (1)$$

Where  $\alpha$  is the propagation loss of the TiO<sub>2</sub>-on-TFLNOI waveguide,  $P_{in}$  is the input signal power,  $P_{out}$  is the output signal power.  $L$  is the total measured length of the waveguide.

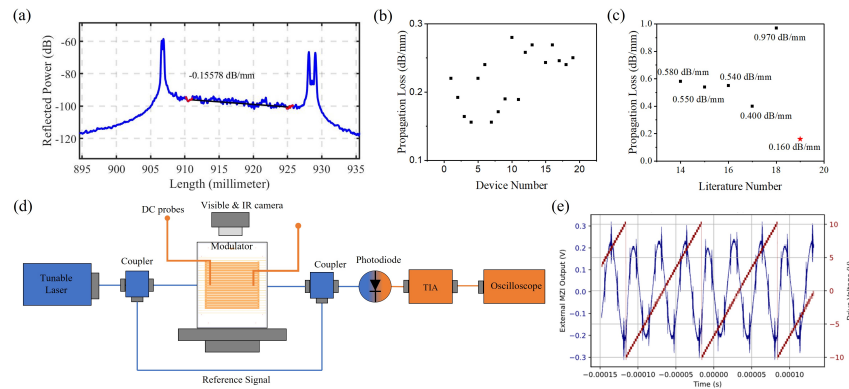


**Fig. 3.** (a): OBR measurement for one of the lowest propagation loss waveguide. (b): All OBR measurements of total 19 waveguides. (c): Comparison between this work and literature [16–20]. (d): The experimental setup for DC modulation testing. (e): The  $V\pi$  trace for TiO<sub>2</sub> phase modulator at 10kHz, 20Vpp. The blue region shows the optical domain, and yellow region shows the electrical domain.

The loss distribution of the whole device was the plot in Fig. 3(b). Because of the nonconformity of the photoresist, the waveguide around the edges has more loss. A scar was observed under the microscope across half of the sample and additional loss was measured caused by the defect. The lowest loss of 0.156 dB/mm was measured by OBR, which is comparable to propagation losses from literature 0.58 dB/mm, 0.54 dB/mm, 0.55 dB/mm, 0.4 dB/mm, 0.97 dB/mm [16–20], as shown in Fig. 3(c). lowest total insertion loss of 13.8 dB was measured for a 2 cm long waveguide. Considering the mode mismatch of fiber-to-waveguide, the result of 5 dB per facet of coupling loss was simulated. The actual coupling loss could be slightly higher because of the imperfect alignment and loss from connectors. By comparing the fiber to fiber measurement and OBR measurement, the proportional loss of the TiO<sub>2</sub>-on-TFLNOI waveguide is around 1-2 dB/cm. Some study have demonstrated that OBR measurement is comparable with cutback method [21]. The OBR measurements requires only one side polishing and coupling loss of the waveguide can be eliminated by calculating the loss difference. Some post-treatments have been studied i.e., wet chemical etching and chemical mechanical polishing, etc., which could smooth the surface and reduce sidewall roughness in future work. A additional layer of sputtered TiO<sub>2</sub> can be added to lower the propagation loss by forming a rib waveguide structure that isolates the optical mode from the surface [9]. The DC- $V\pi$  measurements have been taken to characterize the modulation of this device, shown in Fig. 3(e). Figure 3(d) illustrates the schematic of the electro-optic testing setup, where a 1550 nm single-mode tunable laser was used as a light source and connected with 1 x 2 MMI fiber splitter. The laser was coupled into the waveguide by used polarization maintenance lensed fiber while the DC probe launched on the electrodes. Another reference signal was connected before and recombined after waveguide coupling. The output signal connected with a photodiode, which connected with a trans-impedance amplifier (TIA) then oscilloscope. While sweep the drive voltage from -10 V to 10 V, the voltage caused  $\pi$  phase shift is captured ( $V_\pi$ ). A  $V_\pi$  of 3.2 V and  $V_\pi*L$  of 5.12 were experimentally measured, the noise spike on this plot could be the noise from the TIA. It's a very promising platform by comparing with others' work in following table. This modulation measurement once again proves the feasibility of TiO<sub>2</sub> as a strip loaded waveguide, and shows a potentially good application of TiO<sub>2</sub> in modulators. The high-speed modulator of proposed platform can be achieved by well design the electrodes.

Hybrid TFLN Modulator Comparison			
Material	$V_\pi*L$ (V*cm)	Propagation loss (dB/cm)	Reference
TiO <sub>2</sub> -TFLN	5.12	1.5	This work
Silicon-TFLN	6.7	0.6	[22]
Silicon-TFLN	4.74	5	[23]
SiNx-TFLN	3	7	[24]
SiNx-TFLN	2.11	2.25	[25]
Ta <sub>2</sub> O <sub>5</sub> -TFLN	4	5	[26]

## 5. Conclusion

Presented in this paper is the first TiO<sub>2</sub>-on-TFLNOI hybrid DC EO phase modulator which was designed and fabricated. A bi-layer lift off process and optical lithography were used to define the structures of the optical waveguide and electrode. An optical propagation loss of 0.156 dB/mm and  $V_\pi$  of 3.2 V was measured. The use of TiO<sub>2</sub>-on-TFLNOI hybrid waveguide further expands

the application prospects of lithium niobate and the feasibility of more diverse designs in lithium niobate photonic circuits.

**Funding.** Office of Naval Research (N00014-21-1-2263).

**Acknowledgments.** The authors gratefully acknowledge the Office of Naval Research (ONR) for sponsoring this work, as well as all the help from Phase Sensitive Innovation, inc. and the University of Delaware nanofabrication Facility.

**Disclosures.** The authors declare no conflicts of interest.

**Data availability.** Data underlying the results presented herein are not publicly available at this time but may be obtained from the authors upon reasonable request.

## References

1. Y. Cho and K. Yamanouchi, "Nonlinear, elastic, piezoelectric, electrostrictive, and dielectric constants of lithium niobate," *J. Appl. Phys.* **61**(3), 875–887 (1987).
2. A. J. Mercante, S. Shi, P. Yao, L. Xie, R. M. Weikle, and D. W. Prather, "Thin film lithium niobate electro-optic modulator with terahertz operating bandwidth," *Opt. Express* **26**(11), 14810–14816 (2018).
3. M. Thomaschewski, V. A. Zenin, C. Wolff, and S. I. Bozhevolnyi, "Plasmonic monolithic lithium niobate directional coupler switches," *Nat. Commun.* **11**(1), 748 (2020).
4. S. Nelan, S. Nelan, A. Mercante, C. Hurley, S. Shi, S. Shi, P. Yao, B. Shopp, D. W. Prather, and D. W. Prather, "Compact thin film lithium niobate folded intensity modulator using a waveguide crossing," *Opt. Express* **30**(6), 9193–9207 (2022).
5. A. N. R. Ahmed, S. Shi, A. Mercante, S. Nelan, P. Yao, and D. W. Prather, "High-efficiency lithium niobate modulator for K band operation," *APL Photonics* **5**(9), 091302 (2020).
6. S. Yamabi and H. Imai, "Crystal phase control for titanium dioxide films by direct deposition in aqueous solutions," *Chem. Mater.* **14**(2), 609–614 (2002).
7. T. Jin, J. Zhou, and P. T. Lin, "Mid-infrared electro-optical modulation using monolithically integrated titanium dioxide on lithium niobate optical waveguides," *Sci. Rep.* **9**(1), 15130 (2019).
8. C. J. Tavares, J. Vieira, L. Rebouta, G. Hungerford, P. Coutinho, V. Teixeira, J. O. Carneiro, and A. J. Fernandes, "Reactive sputtering deposition of photocatalytic TiO<sub>2</sub> thin films on glass substrates," *Mater. Sci. Eng., B* **138**(2), 139–143 (2007).
9. I. Hegeman, M. Dijkstra, F. B. Segerink, W. Lee, and S. M. Garcia-Blanco, "Development of low-loss TiO<sub>2</sub> waveguides," *Opt. Express* **28**(5), 5982–5990 (2020).
10. M. R. Saleem, S. Honkanen, and J. Turunen, "Thermal properties of TiO<sub>2</sub> films fabricated by atomic layer deposition," *IOP Conf. Ser.: Mater. Sci. Eng.* **60**, 012008 (2014).
11. F. Qiu, A. M. Spring, and S. Yokoyama, "Athermal and high-Q hybrid TiO<sub>2</sub>-Si<sub>3</sub>N<sub>4</sub> ring resonator via an etching-free fabrication technique," *ACS Photonics* **2**(3), 405–409 (2015).
12. J. Ling, Y. He, R. Luo, M. Li, H. Liang, and Q. Lin, "Athermal lithium niobate microresonator," *Opt. Express* **28**(15), 21682–21691 (2020).
13. C. C. Evans, C. Liu, and J. Suntivich, "Low-loss titanium dioxide waveguides and resonators using a dielectric lift-off fabrication process," *Opt. Express* **23**(9), 11160–11169 (2015).
14. H. D. Jang, S.-K. Kim, and S.-J. Kim, "Effect of particle size and phase composition of titanium dioxide nanoparticles on the photocatalytic properties," *J. Nanopart. Res.* **3**(2/3), 141–147 (2001).
15. M. Lelis, S. Tuckute, S. Varnagiris, M. Urbonavicius, G. Laukaitis, and K. Bockute, "Tailoring of TiO<sub>2</sub> film microstructure by pulsed-DC and RF magnetron co-sputtering," *Surf. Coat. Technol.* **377**, 124906 (2019).
16. S. Li, L. Cai, Y. Wang, Y. Jiang, and H. Hu, "Waveguides consisting of single-crystal lithium niobate thin film and oxidized titanium stripe," *Opt. Express* **23**(19), 24212–24219 (2015).
17. X. Guan, H. Hu, L. K. Oxenløwe, and L. H. Frandsen, "Compact titanium dioxide waveguides with high nonlinearity at telecommunication wavelengths," *Opt. Express* **26**(2), 1055–1063 (2018).
18. K. Hammani, L. Markey, M. Lamy, B. Kibler, J. Arocas, J. Fatome, A. Dereux, J.-C. Weeber, and C. Finot, "Octave spanning supercontinuum in titanium dioxide waveguides," *Appl. Sci.* **8**(4), 543 (2018).
19. J. D. B. Bradley, C. C. Evans, J. T. Choy, O. Reshef, P. B. Deotare, F. Parsy, K. C. Phillips, M. Loncar, and E. Mazur, "Submicrometer-wide amorphous and polycrystalline anatase TiO<sub>2</sub> waveguides for microphotonic devices," *Opt. Express* **20**(21), 23821–23831 (2012).
20. M. Furuhashi, M. Fujiwara, T. Ohshiro, M. Tsutsui, K. Matsubara, M. Taniguchi, S. Takeuchi, and T. Kawai, "Development of microfabricated TiO<sub>2</sub> channel waveguides," *AIP Adv.* **1**(3), 032102 (2011).
21. A. Peczek, C. Mai, G. Winzer, and L. Zimmermann, "Comparison of cut-back method and optical backscatter reflectometry for wafer level waveguide characterization," in *2020 IEEE 33rd International Conference on Microelectronic Test Structures (ICMTS)*, (2020), pp. 1–3. ISSN: 2158–1029.
22. P. O. Weigel, J. Zhao, K. Fang, H. Al-Rubaye, D. Trotter, D. Hood, J. Mudrick, C. Dallo, A. T. Pomerene, A. L. Starbuck, C. T. DeRose, A. L. Lentine, G. Rebeiz, and S. Mookherjee, "Bonded thin film lithium niobate modulator on a silicon photonics platform exceeding 100 GHz 3-dB electrical modulation bandwidth," *Opt. Express* **26**(18), 23728–23739 (2018).

23. Q. Li, H. Zhu, H. Zhang, L. Cai, L. Cai, and H. Hu, "Phase modulators in hybrid silicon and lithium niobate thin films," *Opt. Mater. Express* **12**(4), 1314–1322 (2022).
24. S. Jin, L. Xu, H. Zhang, and Y. Li, "LiNbO<sub>3</sub> thin-film modulators using silicon nitride surface ridge waveguides," *IEEE Photonics Technol. Lett.* **28**(7), 736–739 (2016).
25. A. N. R. Ahmed, S. Nelan, S. Shi, P. Yao, A. Mercante, D. W. Prather, and D. W. Prather, "Subvolt electro-optical modulator on thin-film lithium niobate and silicon nitride hybrid platform," *Opt. Lett.* **45**(5), 1112–1115 (2020).
26. P. Rabiei, J. Ma, S. Khan, J. Chiles, and S. Fathpour, "Heterogeneous lithium niobate photonics on silicon substrates," *Opt. Express* **21**(21), 25573–25581 (2013).